Archive of Applied Mechanics 69 (1999) 555–568 © Springer-Verlag 1999

Control techniques for impacting flexible systems

D. B. Marghitu, C. I. Diaconescu

Summary In this article, a comparative study of the control for the repetitive impacting elastic link with parametrically excited base in rotational motion is considered. First, a sliding mode control strategy based on linearized inverse model is designed and employed to suppress the vibrations of the elastic beam after the impact. The control concept involves the usage of an adaptive plant inverse model as controller in feedforward configurations. Next, a linear controller is designed via Lyapunov-Floquet transformation. In this approach, the time-periodic equations of motion are transformed into a time-invariant form, which is suitable for the application of standard time-invariant controller-design techniques. Finally, a fuzzy logic controller is applied for the nonlinear model of the impacting system. The momentum balance method and an empirical coefficient of restitution is used in the collision.

Key words sliding mode, inverse system, fuzzy logic, coefficient of restitution

1 Introduction

Application of modern control methodology plays a major role in the development of the manipulators, walking machines and robot arms technology. A special attention is paid to the analysis of elastic links that impact rigid surfaces.

An engineering-oriented impact approach for multiple collision industrial applications was developed in [14] using complementary algorithms. The authors replaced the unilateral character of the constraints in the normal direction by an efficient bilateral formulation.

Planar and nonplanar oscillations of a cantilever beam subjected to a planar periodic excitation were studied in [6, 7]. The stability of out-of-plane motion was performed, taking into account damping and geometric nonlinearities in the differential equations of motion.

In [5] an elastic arm was considered, modeled as a pinned-free beam attached to a hub. The objective of the work was to carry out experiments designed to determine the necessary control torque applied at the base of the link using only the tip position measurement. A more complex system was analyzed in [3]. The work was related to the problem of controlling plane rotational motions of two rigid bodies connected by an elastic rod.

The problem of controlling an elastic arm of two links based on variable structure system theory and pole assignment technique for stabilization was treated in [13]. This design approach was motivated by a simple observation that the nonlinearity in the dynamics of an elastic robotics system is essentially due to rigid modes (joint angles), and, as the time derivatives of the rigid modes vanish, the remaining motion is only due to the elasticity. For the rigid modes, a sliding controller was designed. The controller of the elastic modes was constructed using the pole assignment technique. A similar technique is used in [16] to control a flexible/rigid link robot using sliding-mode and a shaped-input controllers. The first controller was used to control the rigid body motion, while the second one served to control the flexible motion. Comparative to the two works above mentioned, the model of the flexible link studied in this paper was improved by considering the axial deformation of the elastic beam. The impact with external bodies or rigid surfaces was also studied. The same sliding mode control

Received 27 January 1999; accepted for publication 3 June 1999

D. B. Marghitu, C. I. Diaconescu
Department of Mechanical Engineering,
Auburn University, AL 36849, USA

strategy was used, but a decoupling controller was designed in order to decouple the global system into several independent equations.

The flap motion control of a rotating flexible beam with a parametrically excited base was studied in [4]. A linear controller, based on Lyapunov-Floquet transformation was constructed to suppress both the deflection angle and the elastic vibrations of the beam. The controller design was based on the idea suggested in [17].

In [15] the control strategy was studied using inversion of multivariable linear system. A new algorithm for constructing an inverse of a multivariable linear dynamic system was developed. This algorithm, which is considerably more efficient than previous methods, also incorporates a relatively simple criterion for determining if the inverse system exists.

A fuzzy logic control scheme to investigate the vibration suppression of a flexible-rod slider mechanism was developed in [2]. A three-mode approximation of the beam was considered. From simulations it was found that the transverse deflection of the flexible link was significantly reduced.

In [9], proportional-integral and fuzzy logic controllers were proposed for a two-link rigid robot. The proportional-integral controller was used to ensure fast transient response and zero steady-state error. The fuzzy logic controller was used to enhance the damping characteristics of the system. However, the author found that the gains adjustment of the proportional-integral controller requires a large effort, and the control scheme does not compensate for the nonlinear effects of the robot system.

In this work, both linear and nonlinear control strategy are applied for the vibration control of a parametrically excited impacted link. An elastic beam is attached to a rigid base which has a parametric excitation. The equations of motion have periodic coefficients. A decoupled controller using sliding-mode strategy is proposed first. The global system is decoupled into several independent components. The inverse system model is used as an actuator for the original system. Next, a controller using Lyapunov-Floquet (L-F) transformation has been designed. Simulated results are provided to demonstrate the applicability of the L-F transformation technique in the study of this class of problems. Finally, a fuzzy-logic controller is implemented to the nonlinear model of the system. Simulations for all control strategies are performed, and their results are shown. Several concluding remarks are presented.

2
System model

In Fig. 1, the slender flexible beam AB is cantilevered onto a rigid massless base with negligible dimensions, [10]. The base is attached to a rigid link OO_1 of variable length $L_0 + L_1 \sin \omega t$ with negligible mass. The flexible beam has the length L, a constant flexural rigidity EI and a uniformly distributed mass per unit length $\rho = m/L$, where m is the total mass of the beam. The base can perform small rotational deflections $\phi(t)$. A spring of constant k and a damper of constant c are connected to the base and the rigid link in order to avoid large rotation of ϕ. The whole system rotates with a constant angular velocity Ω in the horizontal plane.

The impacted rigid link of length l_b and mass m_b can rotate around the fixed point S. The rigid link is connected to the ground through a spring of constant k_b and a damper of constant c_b,

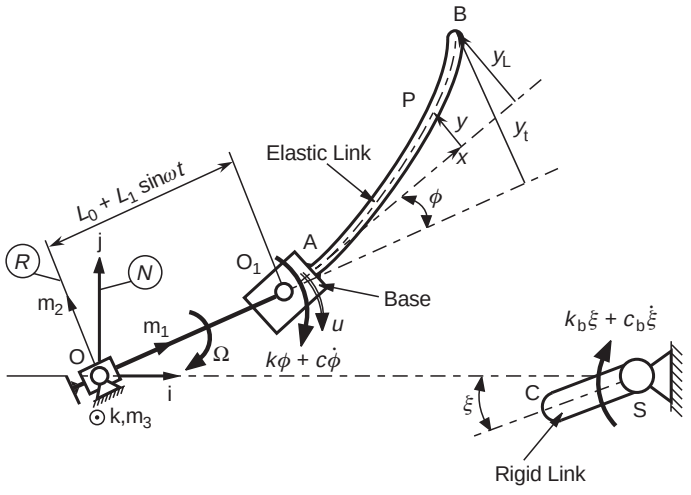

Fig. 1. Parametrically excited impacting system

avoiding large values of the angle ξ. The spring and the damper are designed such that, after each impact between the two links, the angle ξ goes rapidly to zero before a new impact occurs.

Two reference frames are considered: a "fixed" reference frame (N) of unit vectors **i, j** and **k**, whose origin is at O, and a rotating reference frame (R) of unit vectors $\mathbf{m}_1$, $\mathbf{m}_2$ and $\mathbf{m}_3$, with the origin at O and attached to the rigid link OO_1. The unit vectors are related by the transformation

$$\begin{bmatrix} \mathbf{m}_1 \\ \mathbf{m}_2 \\ \mathbf{m}_3 \end{bmatrix} = \begin{bmatrix} \cos\Omega t & \sin\Omega t & 0 \\ -\sin\Omega t & \cos\Omega t & 0 \\ 0 & 0 & 1 \end{bmatrix} \begin{bmatrix} \mathbf{i} \\ \mathbf{j} \\ \mathbf{k} \end{bmatrix} \quad . \tag{1}$$

Let x be the position of any point P on the elastic beam with respect to the end A of the base, and y be the elastic deflection. The position vector of the point P is

$$\mathbf{r}_P = (L_0 + L_1 \sin\omega t + x\cos\phi - y\sin\phi)\mathbf{m}_1 + (y\cos\phi + x\sin\phi)\mathbf{m}_2 \quad . \tag{2}$$

The elastic deflection y of the beam is computed as

$$y(x,t) = \sum_{i=1}^{n} \Psi_i(x) q_i(t) \quad , \tag{3}$$

where $q_i(t)$ are the generalized elastic coordinates and $n \in \mathcal{N}$ is the total number of vibrational modes ($\mathcal{N}$ is the set of natural numbers). The functions $\Psi_i(x)$ are chosen as the mode shapes of a cantilever beam and are defined by the expression

$$\Psi_i(x) = \cosh(z) - \cos(z) - \frac{\cosh(\lambda_i) + \cos(\lambda_i)}{\sinh(\lambda_i) + \sin(\lambda_i)} [\sinh(z) - \sin(z)] \quad , \tag{4}$$

where

$$z = \frac{x\lambda_i}{L} \quad , \tag{5}$$

and λ_i ($i = 1, \ldots, n$) are the first nth consecutive roots of the transcendental equation

$$\cos(\lambda)\cosh(\lambda) = -1 \quad . \tag{6}$$

The additional degree of freedom of the flexible link is due to the rotation $\phi(t)$ of the base. The transverse elastic deflection of the end B with respect to the base axis is y_L, and the total deformation of the same tip with respect to $\mathbf{m}_1$ unit vector is y_t, Fig. 1.

The velocity of the point P in the fixed reference frame (N) is computed with the expression

$$\mathbf{v}_P = \frac{{}^R\mathrm{d}\mathbf{r}_P}{\mathrm{d}t} + \boldsymbol{\Omega} \times \mathbf{r}_P \quad , \tag{7}$$

where the first term of the right-hand side represents the derivative with respect to time in the moving reference frame (R), and $\boldsymbol{\Omega} = -\Omega\mathbf{k}$.

The total kinetic energy of the system is

$$K = \frac{\rho}{2}\int_0^L \mathbf{v}_P \cdot \mathbf{v}_P \, \mathrm{d}x + \frac{m_b l_b^2 \dot{\xi}^2}{6} \quad . \tag{8}$$

The total potential energy of the system is computed as

$$U = \frac{EI}{2}\int_0^L \frac{\partial^2 y}{\partial x^2}\mathrm{d}x + \frac{1}{2}k\phi^2 + \frac{1}{2}k_b\xi^2 \quad . \tag{9}$$

Using Lagrange's method, the nonlinear equations of motion are of the form

$$\mathbf{M}(\mathbf{x})\ddot{\mathbf{x}} + \mathbf{f}(\mathbf{x}, t) = \mathbf{d}u \ , \tag{10}$$

where $\mathbf{x}$ is the generalized coordinates vector, defined by $\mathbf{x} = [\phi, q_1, q_2, q_3, \xi]^{\mathrm{T}}$, $\mathbf{M}(\mathbf{x})$ is the mass matrix, $\mathbf{f}(\mathbf{x}, t)$ is a nonlinear vector, which contains periodic coefficients, $\mathbf{d} = [1, 0, 0, 0, 0]^{\mathrm{T}}$ is the input vector, and u is the control torque applied to the moving base, as shown in Fig. 1. For the simulations presented here, a three-mode approximation ($n = 3$) is used. The nonlinear equations of motion are linearized around the zero equilibrium position $\phi = q_1 = q_2 = q_3 = \xi = 0$. The matrix form of the linearized equations of motion is

$$\mathbf{M}\ddot{\mathbf{x}}(t) + \mathbf{C}\dot{\mathbf{x}}(t) + [\mathbf{K} + \mathbf{V}(t)]\mathbf{x}(t) = \mathbf{d}u(t) \ . \tag{11}$$

The various coefficients involved in the linearized equation of motion (11) are

- The mass matrix

$$\mathbf{M} = \begin{bmatrix} \frac{mL^2}{3} & F_1 & F_2 & F_3 & 0 \\ F_1 & G_1 & 0 & 0 & 0 \\ F_2 & 0 & G_2 & 0 & 0 \\ F_3 & 0 & 0 & G_3 & 0 \\ 0 & 0 & 0 & 0 & \frac{m_b l_b^2}{3} \end{bmatrix} , \tag{12}$$

- The damping matrix

$$\mathbf{C} = \begin{bmatrix} c & 0 & 0 & 0 & 0 \\ 0 & 0 & 0 & 0 & 0 \\ 0 & 0 & 0 & 0 & 0 \\ 0 & 0 & 0 & 0 & 0 \\ 0 & 0 & 0 & 0 & c_b \end{bmatrix} , \tag{13}$$

- The constant part of the stiffness matrix defined as

$$\mathbf{K} = \begin{bmatrix} k + L_1\Omega^2 m\frac{L}{2} & L_1\Omega^2 V_1 & L_1\Omega^2 V_2 & L_1\Omega^2 V_3 & 0 \\ L_1\Omega^2 V_1 & \alpha_1 & 0 & 0 & 0 \\ L_1\Omega^2 V_2 & 0 & \alpha_2 & 0 & 0 \\ L_1\Omega^2 V_3 & 0 & 0 & \alpha_3 & 0 \\ 0 & 0 & 0 & 0 & k_b \end{bmatrix} , \tag{14}$$

where $\alpha_i = -m\Omega^2 G_i + EIH_i/L^3$, $i = 1, 2, 3$.

- The periodic part of the stiffness matrix defined as

$$\mathbf{V}(t) = L_0(\Omega^2 + \omega^2) \begin{bmatrix} \frac{mL}{2} & V_1 & V_2 & V_3 & 0 \\ V_1 & 0 & 0 & 0 & 0 \\ V_2 & 0 & 0 & 0 & 0 \\ V_3 & 0 & 0 & 0 & 0 \\ 0 & 0 & 0 & 0 & 0 \end{bmatrix} \sin\omega t \ . \tag{15}$$

Functions F_i , G_i , V_i and H_i ($i = 1, 2, 3$) are defined as

$$F_i = \int_0^L x\rho\Psi_i(x)\mathrm{d}x, \quad G_i = \int_0^L \rho\Psi_i^2(x)\mathrm{d}x,$$
$$V_i = \int_0^L \rho\Psi_i(x)\mathrm{d}x, \quad H_i = \int_0^L \left(\frac{\partial\Psi_i(x)}{\partial x}\right)^2 \mathrm{d}x \ . \tag{16}$$

In state space form, Eq. (11) can be written as

$$\dot{\boldsymbol{\varepsilon}}(t) = \mathbf{A}(t)\boldsymbol{\varepsilon}(t) + \mathbf{b}u(t) \ , \tag{17}$$

where $\boldsymbol{\varepsilon}(t) = [\mathbf{x}(t), \dot{\mathbf{x}}(t)]^{\mathrm{T}}$ is the state space vector. Matrices $\mathbf{A}(t)$ and $\mathbf{b}$ are defined as

$$\mathbf{A}(t) = \begin{bmatrix} \mathbf{0}_{5\times5} & \mathbf{I}_{5\times5} \\ -\mathbf{M}^{-1}(\mathbf{K}+\mathbf{V}(t)) & -\mathbf{M}^{-1}\mathbf{C} \end{bmatrix}, \quad \mathbf{b} = \begin{bmatrix} \mathbf{0}_5 \\ \mathbf{M}^{-1}\mathbf{d} \end{bmatrix} \ , \tag{18}$$

where $\mathbf{0}_{5\times5}$ and $\mathbf{I}_{5\times5}$ are the zero and the identity matrices of order five, respectively, and $\mathbf{0}_5$ is a 5×1 zero vector. Matrix $\mathbf{A}(t)$ is periodic with period $T = 2\pi/\omega$.

3
Impact equations

The equations of impulsive motion are determined following the procedure described in [12]. A basic assumption is that the configuration of the bodies is held constant in the analysis of the collision process, with no significant change in mass and moments of inertia. Let $\mathbf{F}_c$ be the impact force, which in this case has only a component in $\mathbf{i}$ direction

$$\mathbf{F}_c = [0, F_c, 0] \ . \tag{19}$$

The friction during the impact is neglected. Let $\mathbf{v}$ be the vector of generalized speed defined as

$$\mathbf{v} = \left[\dot{\phi}, \dot{q}_1, \dot{q}_2, \dot{q}_3, \dot{\xi}\right]^{\mathrm{T}} = \left[v_j\right]_{j=1,2,3,4,5} \ . \tag{20}$$

An integrated form of the differential equations is

$$\frac{\mathrm{d}}{\mathrm{d}t}\frac{\partial K}{\partial v_j} = Q_j \ , \tag{21}$$

where Q_j are the generalized impulsive forces during impact. Equation (21) establishes a relationship between the time derivative of the generalized vector $\mathbf{v}$ and the contact force F_c, which leads to the matrix form

$$\mathbf{M}\mathbf{v} = \mathbf{D}(\mathbf{x})F_c \ , \tag{22}$$

where $\mathbf{D}(\mathbf{x})$ is a vector that depends on pre-impact positions. Because at the impact moment ξ can be expressed in terms of ϕ, q_1, q_2 and q_3, only the first four components of the generalized vector $\mathbf{v}$ are independent.

Let $\mathbf{v}_B^-$ and $\mathbf{v}_B^+$ be the velocities of the elastic beam tip before and after impact, respectively. Let $\mathbf{v}_C^-$ and $\mathbf{v}_C^+$ be the velocities of the impacted rigid end link before and after impact, respectively. With these notations, one can write

$$\mathbf{v}_C^+ - \mathbf{v}_B^+ = e(\mathbf{v}_B^- - \mathbf{v}_C^-) \ , \tag{23}$$

where e is the kinematic coefficient of restitution. By solving the system of equations (22) and (40), the unknown velocities after impact $[\dot{\phi}^+, \dot{q}_1^+, \dot{q}_2^+, \dot{q}_3^+, \dot{\xi}^+]$ are determined.

4
Controller design

4.1
Sliding mode controller

A sliding-mode control procedure based on usage of inverse model and a decoupled control system, Fig. 2, is proposed in order to eliminate the vibration of the elastic beam, [11]. The

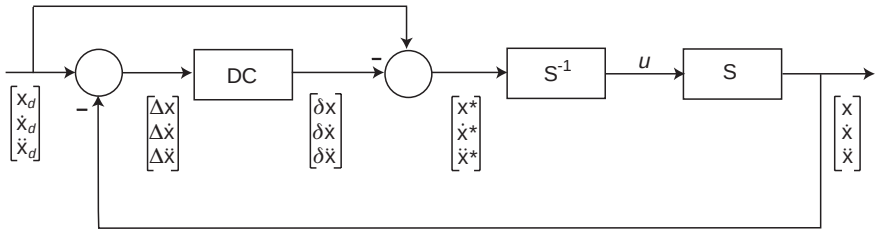

Fig. 2. Basic configuration of the sliding-mode control system

control method uses an inverse model $\mathbf{S}^{-1}$ of the original (direct) model $\mathbf{S}$ and a Decoupling Controller (DC) which separates the global system into several independent components. The inverse model has a transfer function like the reciprocal of the plant transfer function and becomes the controller for the original model. Let consider $\mathbf{x}_d(t)$, $\dot{\mathbf{x}}_d(t)$ and $\ddot{\mathbf{x}}_d(t)$ be the vectors which represent the desired position, velocity and acceleration of the impacting system, and $\mathbf{x}(t)$, $\dot{\mathbf{x}}(t)$ and $\ddot{\mathbf{x}}(t)$ be the measured values.

The errors of this control system are

$$\Delta\mathbf{x} = \mathbf{x}_d - \mathbf{x}, \quad \Delta\dot{\mathbf{x}} = \dot{\mathbf{x}}_d - \dot{\mathbf{x}}, \quad \Delta\ddot{\mathbf{x}} = \ddot{\mathbf{x}}_d - \ddot{\mathbf{x}} \ , \tag{24}$$

The controller will generate new variations $\delta\mathbf{x}$, $\delta\dot{\mathbf{x}}$, $\delta\ddot{\mathbf{x}}$

$$\begin{bmatrix} \delta\mathbf{x} \\ \delta\dot{\mathbf{x}} \\ \delta\ddot{\mathbf{x}} \end{bmatrix} = \mathbf{R} \begin{bmatrix} \Delta\mathbf{x} \\ \Delta\dot{\mathbf{x}} \\ \Delta\ddot{\mathbf{x}} \end{bmatrix} \ , \tag{25}$$

where $\mathbf{R}$ is a (15×15)-dimensional matrix which defines the control law and assures the decoupling of the system. This matrix will be presented later on.

The new variations $\delta\mathbf{x}$, $\delta\dot{\mathbf{x}}$, $\delta\ddot{\mathbf{x}}$ generate a new trajectory

$$\mathbf{x}^* = \mathbf{x}_d - \delta\mathbf{x}, \quad \dot{\mathbf{x}}^* = \dot{\mathbf{x}}_d - \delta\dot{\mathbf{x}}, \quad \ddot{\mathbf{x}}^* = \ddot{\mathbf{x}}_d - \delta\ddot{\mathbf{x}} \ , \tag{26}$$

which is used as a reference trajectory for the inverse system ($\mathbf{S}^{-1}$).

The equations which describe the direct and inverse system are

$$\mathbf{M}(\ddot{\mathbf{x}}_d - \Delta\ddot{\mathbf{x}}) + \mathbf{C}(\dot{\mathbf{x}}_d - \Delta\dot{\mathbf{x}}) + (\mathbf{K} + \mathbf{V}\sin\omega t)(\mathbf{x}_d - \Delta\mathbf{x}) = \mathbf{d}u \ , \tag{27}$$

$$\mathbf{M}(\ddot{\mathbf{x}}_d - \delta\ddot{\mathbf{x}}) + \mathbf{C}(\dot{\mathbf{x}}_d - \delta\dot{\mathbf{x}}) + (\mathbf{K} + \mathbf{V}\sin\omega t)(\mathbf{x}_d - \delta\mathbf{x}) = \mathbf{d}u \ . \tag{28}$$

BY subtracting Eq. (27) from Eq. (28), the dynamic model of the direct and inverse system developed around the reference trajectory $\mathbf{x}_d$, $\dot{\mathbf{x}}_d$, $\ddot{\mathbf{x}}_d$ can be rewritten as

$$\mathbf{M}(\Delta\ddot{\mathbf{x}} - \delta\ddot{\mathbf{x}}) + \mathbf{C}(\Delta\dot{\mathbf{x}} - \delta\dot{\mathbf{x}}) + (\mathbf{K} + \mathbf{V}\sin\omega t)(\Delta\mathbf{x} - \delta\mathbf{x}) = 0 \ . \tag{29}$$

The matrix $\mathbf{R}$ has the following form:

$$\mathbf{R} = \begin{bmatrix} \mathbf{R}_3 & 0 & 0 \\ 0 & \mathbf{R}_2 & 0 \\ \mathbf{P}_2 + \mathbf{P}_3\sin\omega t & \mathbf{P}_1 & \mathbf{R}_1 \end{bmatrix} \ , \tag{30}$$

and it is selected such that

$$\delta\ddot{\mathbf{x}} = \mathbf{R}_1\Delta\ddot{\mathbf{x}} + \mathbf{P}_1\Delta\dot{\mathbf{x}} + \mathbf{P}_2\Delta\mathbf{x} + \mathbf{P}_3\sin\omega t\Delta\mathbf{x} \ , \tag{31}$$

$$\delta\dot{\mathbf{x}} = \mathbf{R}_2\Delta\dot{\mathbf{x}} \ , \tag{32}$$

$$\delta\mathbf{x} = \mathbf{R}_3\Delta\mathbf{x} \ . \tag{33}$$

Matrices $\mathbf{P}_i$, $\mathbf{R}_i$ are chosen to verify the relations

$$\mathbf{R}_1 = \mathbf{M}^{-1}(\mathbf{M} - \mathbf{I}) \ , \tag{34}$$

$$\mathbf{R}_3 = -\alpha\mathbf{I} \ , \tag{35}$$

$$\mathbf{P}_3 = \mathbf{M}^{-1}[(\alpha + 1)\mathbf{V} - \mathbf{D}] \ , \tag{36}$$

$$\mathbf{P}_2 = \mathbf{M}^{-1}[(\alpha + 1)\mathbf{K} - \mathbf{B}] \ , \tag{37}$$

$$\mathbf{C}(\mathbf{I} - \mathbf{R}_2) - \mathbf{M}\mathbf{P}_1 = 2\mathbf{Z} \ , \tag{38}$$

where $\alpha = 2, 3, \ldots$

In order to assure the decoupling of the system of equations, the matrices **D**, **B** and **Z** are chosen of the diagonal form as follows

$$\mathbf{D} = \mathrm{diag}(d_1, d_2, d_3, d_4, d_5) \ , \tag{39}$$

$$\mathbf{B} = \mathrm{diag}(b_1, b_2, b_3, b_4, b_5) \ , \tag{40}$$

$$\mathbf{Z} = \mathrm{diag}(\zeta_1, \zeta_2, \zeta_3, \zeta_4, \zeta_5) \ . \tag{41}$$

Equation (29) becomes

$$\Delta\ddot{\mathbf{x}} + 2\mathbf{Z}\Delta\dot{\mathbf{x}} + (\mathbf{B} + \mathbf{D}\sin\omega t)\Delta\mathbf{x} = 0 \ , \tag{42}$$

Equation (42) can be rewritten as a set of five independent equations

$$\Delta\ddot{\mathbf{x}} + 2\zeta_i\Delta\dot{\mathbf{x}} + (b_i + d_i\sin\omega t)\Delta\mathbf{x} = 0 \ , \tag{43}$$

for $i = 1, 2, 3, 4, 5$. These equations represent the decoupled equations of the errors for the original system.

A sliding mode controller is designed using the damping coefficient ζ_i as control variable. The control of the motion is divided in two parts. During the first part the controller assures the motion toward the switching line, and in the second part the motion is forced along the switching line by the control of the damping coefficients ζ_i in Eq. (42). The switching line is defined as follows:

$$\Delta\dot{\mathbf{x}}_i + f_i\Delta\mathbf{x}_i = 0 \ , \tag{44}$$

and the control law is defined by

$$\zeta_i < m_i, \zeta_i > M_i \ , \tag{45}$$

to assure the stable evolution of the system, where m_i and M_i are defined as follows:

$$m_i = \min(b_i + d_i\sin\omega t)^{1/2}, \quad M_i = \max(b_i + d_i\sin\omega t)^{1/2} \tag{46}$$

4.2
State feedback controller

Returning back to Eq. (17), the objective is to determine a linear time-varying control law of the type

$$u = \mathbf{F}\boldsymbol{\varepsilon} \ , \tag{47}$$

where **F** is the feedback matrix. It is assumed that all states are available for control, by measurement. The controller design is based on Lyapunov-Floquet transformation, and the procedure developed in [17] is applied.

To determine the Lyapunov-Floquet transformation, one must first compute the fundamental matrix (or state transition matrix) $\boldsymbol{\Phi}(t)$. This can be done either analytically, using the Chebyshev polynomials expansion approach, [8], or by numerical integration of the matrix differential equation

$$\dot{\boldsymbol{\Phi}}(t) = \mathbf{A}(t)\boldsymbol{\Phi}(t), \quad 0 < t \leq T \ , \tag{48}$$

with the initial condition

$$\boldsymbol{\Phi}(0) = \mathbf{I}_5 \ . \tag{49}$$

For a time $t_1 > T$, the state transition matrix can be computed using the expression

$$\boldsymbol{\Phi}(t_1) = \boldsymbol{\Phi}(t + rT) = \boldsymbol{\Phi}(t)\boldsymbol{\Phi}^r(T) \ , \tag{50}$$

where r is a suitable integer, and $\mathbf{\Phi}(T)$ is the state transition matrix evaluated at the end of the principal period. This matrix is also called Floquet Transition Matrix (FTM). Matrix $\mathbf{\Phi}(t)$ can be factored as

$$\mathbf{\Phi}(t) = \mathbf{Q}(t)e^{\mathbf{R}t} \quad , \tag{51}$$

where $\mathbf{Q}(t)$ is a $2T$ real periodic matrix, and $\mathbf{R}$ is a real constant matrix. Due to the periodicity of the matrix $\mathbf{Q}(t)$, matrix $\mathbf{R}$ is computed using the expression

$$\mathbf{R} = \frac{1}{2T}\ln \mathbf{\Phi}(2T) = \frac{1}{2T}\ln \mathbf{\Phi}^2(T) \quad . \tag{52}$$

Applying the Lyapunov-Floquet transformation

$$\boldsymbol{\varepsilon}(t) = \mathbf{Q}(t)\mathbf{z}(t) \quad , \tag{53}$$

to Eq. (17), the following system is obtained:

$$\dot{\mathbf{z}}(t) = \mathbf{R}\mathbf{z}(t) + \mathbf{Q}^{-1}(t)\mathbf{b}u(t) \quad . \tag{54}$$

At this point, an auxiliary time invariant system of the type

$$\dot{\bar{\mathbf{z}}}(t) = \mathbf{R}\bar{\mathbf{z}}(t) + \mathbf{B_o}\mathbf{v}(t) \quad , \tag{55}$$

is constructed. In Eq. (55), $\mathbf{B_o}$ is a full rank constant matrix, such that the pair $(\mathbf{R}, \mathbf{B_o})$ is controllable. The control vector $\mathbf{v}(t)$ of the system given by Eq. (55) is determined by designing a full-state feedback controller, using either the pole placement technique or the optimal control theory. Thus one can write

$$\mathbf{v}(t) = \mathbf{F_o}\bar{\mathbf{z}}(t) \quad , \tag{56}$$

where $\mathbf{F_o}$ is a constant feedback gain. Defining $\mathbf{e}(t) \equiv \mathbf{z}(t) - \bar{\mathbf{z}}(t)$, the dynamic error between the state vectors $\mathbf{z}$ and $\bar{\mathbf{z}}$, Eqs. (54) and (55) yield

$$\dot{\mathbf{e}}(t) = (\mathbf{R} + \mathbf{B_o}\mathbf{F_o})\mathbf{e}(t) + \mathbf{Q}^{-1}(t)\mathbf{b}u(t) - \mathbf{B_o}\mathbf{F_o}\mathbf{z}(t) \quad . \tag{57}$$

Since $(\mathbf{R} + \mathbf{B_o}\mathbf{F_o})$ is the stability matrix, the systems defined by Eqs. (54) and (55) can be made equivalent if

$$\mathbf{Q}^{-1}(t)\mathbf{b}u(t) = \mathbf{B_o}\mathbf{F_o}\mathbf{z}(t) \quad . \tag{58}$$

Because condition (58) can not be exactly satisfied, these systems are made equivalent in the least-square sense. For this purpose, first the error vector is defined as

$$\boldsymbol{\eta} = \mathbf{b}u(t) - \mathbf{Q}(t)\mathbf{B_o}\mathbf{F_o}\mathbf{z}(t) \quad , \tag{59}$$

and $u(t)$ is computed such that the performance index $\boldsymbol{\eta}^T\boldsymbol{\eta}$ is minimized. This procedure yields, [17]

$$u(t) = \mathbf{b}^*\mathbf{Q}(t)\mathbf{B_o}\mathbf{F_o}\mathbf{z}(t) \quad , \tag{60}$$

where $\mathbf{b}^*$ is the generalized inverse of matrix $\mathbf{b}$, defined as

$$\mathbf{b}^* = (\mathbf{b}^{\mathrm{T}}\mathbf{b})^{-1}\mathbf{b}^{\mathrm{T}} \quad . \tag{61}$$

Applying the inverse Lyapunov-Floquet transformation to Eq. (60), we obtain

$$u(t) = \mathbf{b}^*\mathbf{Q}(t)\mathbf{B_o}\mathbf{F_o}\mathbf{Q}^{-1}(t)\boldsymbol{\varepsilon}(t) \quad . \tag{62}$$

Comparing Eq. (62) with Eq. (47), the desired feedback gain matrix $\mathbf{F}(t)$ is

$$\mathbf{F}(t) = \mathbf{b}^*\mathbf{Q}(t)\mathbf{B_o}\mathbf{F_o}\mathbf{Q}^{-1}(t) \quad . \tag{63}$$

It should be observed that the feedback matrix from Eq. (63) can be computed off line and stored into the computer memory, since $\mathbf{Q}(t)$ and $\mathbf{Q}^{-1}(t)$ are $2T$-periodic and information for $t > 2T$ is not needed. This is important for a real-time implementation of the control algorithm.

4.3
Fuzzy-logic controller

In this Section, a fuzzy-logic controller for the nonlinear system is designed such that the elastic vibration of the beam are eliminated. The total deflection y_t of the beam tip can be computed with the expression $y_t = L\sin\phi + y_L\cos\phi$, where y_L is the elastic deflection of the beam tip, computed as

$$y_L(t) = y(L,t) = \sum_{i=1}^{3} \Psi_i(L) q_i(t) \quad . \tag{64}$$

The inputs of the fuzzy-logic controller are the total deflection y_t and its time derivative $\dot{y}_t$. The output of the controller is the torque u applied to the base of the elastic link.

Figure 3a shows the fuzzy sets for the total beam deflection y_t (μ_{y_t}). There are seven grades, that correspond to negative huge (NH), negative big (NB), negative small (NS), zero (ZE), positive small (PS), positive big (PB), and positive huge (PH) values of the total beam deflection y_t. One can see that the support vector of y_t is between -1 and 1 m. However, the total deflection y_t is not restricted to belong to this support, by extending the fuzzy set to $\pm\infty$. This means that, for instance, any deflection larger than 1 m will belong to the positive huge (PH) set.

The fuzzy sets of the time derivative $\dot{y}_t$, are represented in Fig. 3b. It has only three grades, which correspond to negative (N), zero (Z), and positive (P) values of $\dot{y}_t$. The support vector is taken between -2 and 2 m/s, but $\dot{y}_t$ can have any value, by extension.

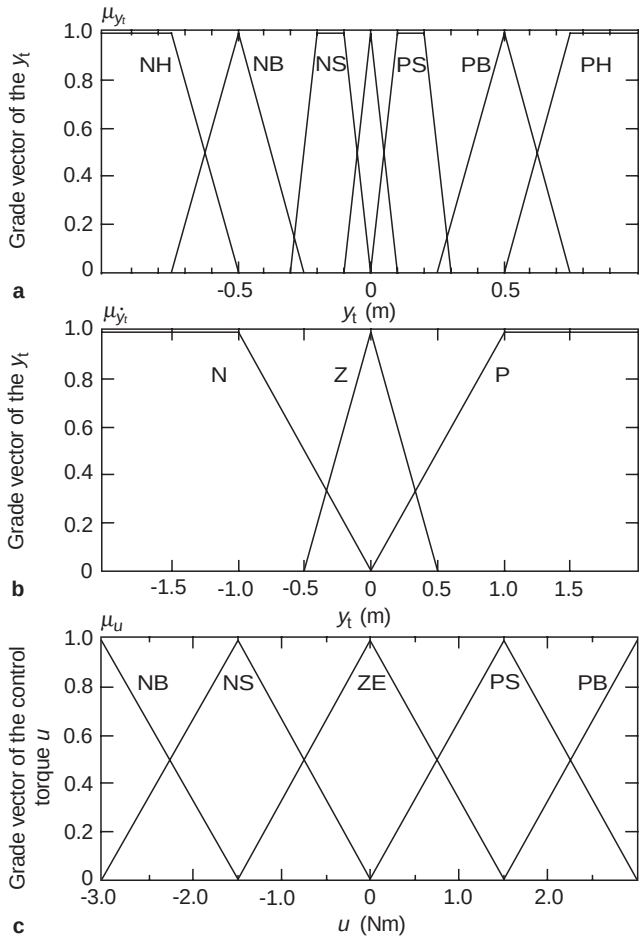

Fig. 3a–c. Fuzzy sets of the fuzzy-logic controller inputs and outputs

Table 1. The consequent table for fuzzy-logic controller design

y_t	NH	NB	NS	ZE	PS	PB	PH
$\dot{y}_t$=N	PB	PS	PS	ZE	ZE	NS	NB
$\dot{y}_t$=Z	PS	PS	ZE	ZE	ZE	NS	NS
$\dot{y}_t$=P	PB	PS	ZE	ZE	NS	NS	NB

The fuzzy sets of the controller output u are shown in Fig. 3c. It consists of equidistant triangle grades. The control force fuzzy set has five components, that correspond to negative big (NB), negative small (NS), zero (ZE), positive small (PS), positive big (PB) values of the controller output.

The controller output is generated using "If-Then" rules, based on a consequent table. The "If-Then" rule has two parts, an antecedent and a consequent. The antecedent is the "If" part, and the consequent is the "Then" part. The consequent table (defined in Table 1) is a matrix of seven columns (the number of grades of y_t fuzzy set) and three rows (the number of grades of $\dot{y}_t$ fuzzy set). Each time, according to the values of y_t and $\dot{y}_t$, one or more "If-Then" rules may be defined. The computation of the control torque u is also based on the intersection and union of fuzzy sets, as well as on the centroid method that returns the "center of mass" of a fuzzy set, [1].

5 Results

For the system shown in Fig. 1, a parametric excitation of amplitude $L_1 = 0.002$ m and frequency $\omega = 10$ rad/s is considered. The distance between the massless base O_1 and the rotation center O is $OO_1 = L_0 + L_1 \sin \omega t$, where $L_0 = 0.02$ m. The system is rotating with a constant angular velocity $\Omega = 1$ rad/s. The value of the spring constant and damping constant are $k = 5.0$ Nm/rad and $c = 2.0$ Nms/rad, respectively. Simulations are performed for elastic link of length $L = 1.5$ m. The mass/unit length of the elastic link is $\rho = 0.612$ kg/m, and the mass of the impacted rigid link is $m_b = 0.3$ kg. The values of the spring and damping constant used for impacted link are $k_b = 10$ Nm/rad and $c_b = 5.0$ Nms/rad, respectively. A kinematic coefficient of restitution $e = 0.5$ for the elasto-plastic impact of the two bodies is considered. The values of the various coefficients involved in the equations of motion are shown in Table 2.

Computer programs are developed to simulate the impact of the elastic beam with the rigid link. The evolution of the uncontrolled and controlled system is studied. The behavior of the uncontrolled system is depicted in Fig. 4. The beam deflection y_t is presented in Fig. 4a, while Fig. 4b shows the evolution of the angle ϕ. Due to the damping, the magnitude of the oscillations decreases in time, but does not vanish.

The behavior of the controlled system using a sliding-mode strategy is presented in Fig. 5. For the sliding-mode control procedure, the diagonal elements of the matrices **D** and **B** are $d_i = 3$, $b_i = 5$ for $i = 1, 2, \ldots, 5$. The evolution of the beam deflection is depicted in Fig. 5a. Due to the control torque applied on the massless base of the elastic beam, the deflection of the beam vanishes in less than 5 s, and is zero at the following impact moment (not shown in the picture). The evolution of the angle ϕ is depicted in Fig. 5b, while the control torque u is represented in Fig. 5c. A maximum value of $u = -2.7$ Nm is noticed after the impact moment.

Figure 6 shows the phase portrait for the angle ϕ and beam deflection y_t for the sliding mode controlled system. The system evolves from the zero state, which characterized the system before the impact moment. Due to the impact with the rigid link, a jump in the state of the system is noticed. After the impact, the system evolves to the switching line, and follows this line until the zero state is reached.

The behavior of the controlled system using state feedback controller is presented in Fig. 7. The maximum value of the beam deflection depicted in Fig. 7a is $y_t = 0.125$ m. The deflection y_t vanishes before a new impact occurs. Figure 7b shows the behavior of the angle ϕ. After

Table 2. The values of the coefficients involved in the equation of motion (11)

	F_1 [Kg m]	F_2 [Kg m]	F_3 [Kg m]	G_1 [Kg]	G_2 [Kg]	G_3 [Kg]	H_1 [m^{-1}]	H_2 [m^{-1}]	H_3 [m^{-1}]	V_1 [Kg]	V_2 [Kg]	V_3 [Kg]
$L = 1.5$ m	0.7840	0.1251	0.0446	0.9189	0.9189	0.9189	3.6629	143.8574	1127.8655	0.7195	0.3987	0.2337

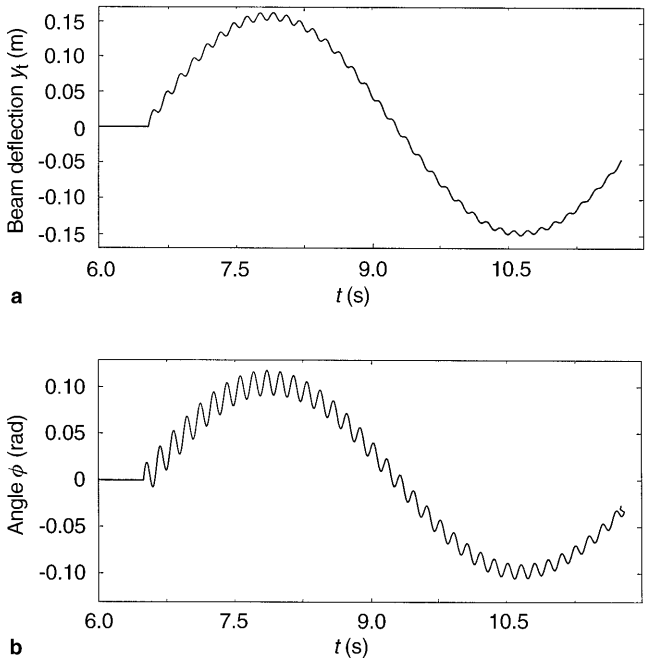

Fig. 4a, b. Uncontrolled system behavior

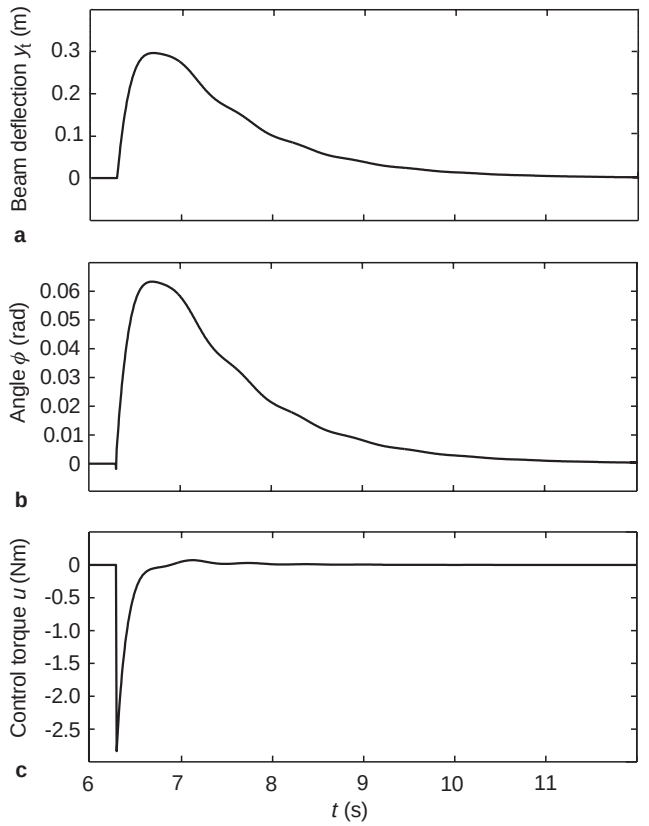

Fig. 5a–c. Controlled system using sliding-mode strategy

impact, a maximum value of 0.085 rad is noticed, but ϕ goes to zero in a short time. Figure 7c represents the applied control torque. The control torque u has a large peak value immediately after impact, and then it goes to zero in a very short time interval.

Figure 8 shows the evolution of the fuzzy-logic controlled system. The total beam tip deflection y_t, Fig. 8a, as well as the angle ϕ, Fig. 8b, vanish in less than 2 s after the impact moment. A maximum peak $y_t = 0.035$ m is noticed. The angle ϕ has a negative jump at the impact moment. The control torque applied on the massless base is depicted in Fig. 8c. It has a maximum value of -2.7 Nm, and vanishes in a short period of time.

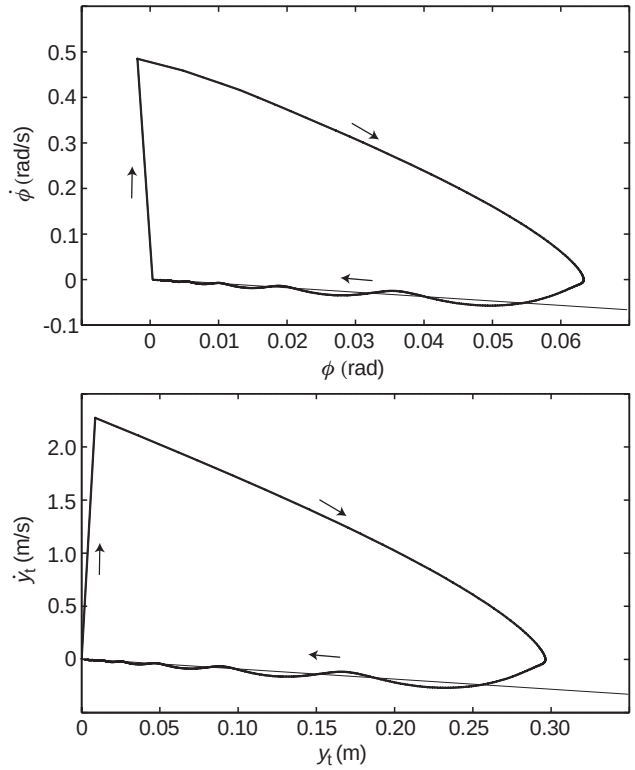

Fig. 6a, b. Phase portrait of beam deflection y_t and angle ϕ for sliding-mode controlled system

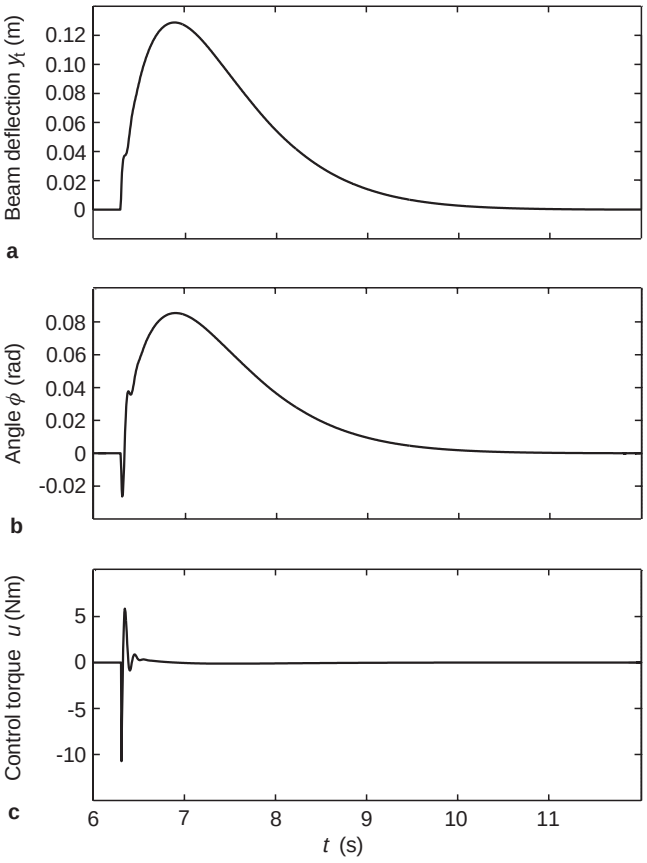

Fig. 7a–c. Controlled system using Lyapunov-Floquet transformation technique

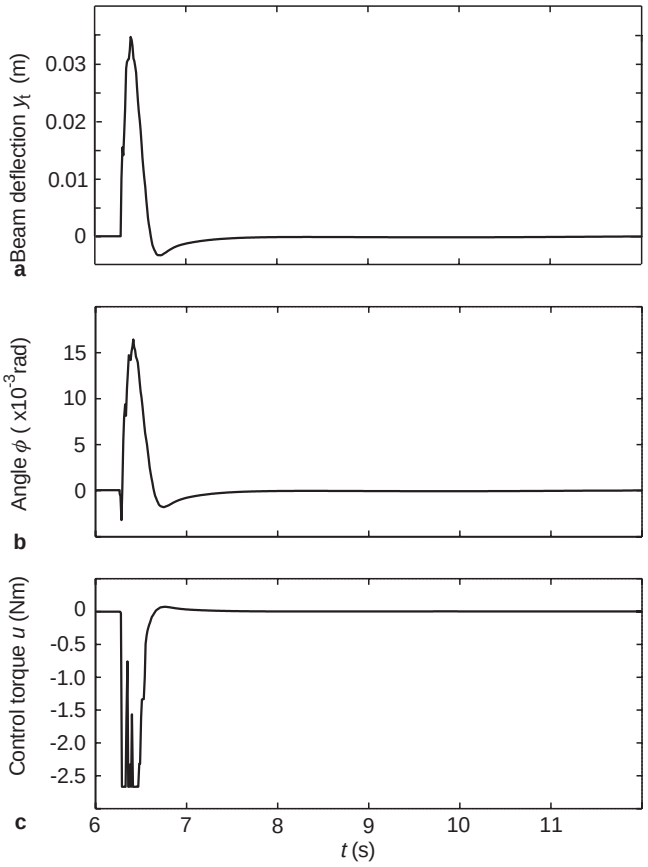

Fig. 8a–c. Controlled system using fuzzy-logic strategy

6 Conclusions

The control problem associated with a parametrically excited rotating flexible link impacting periodically with a rigid beam is studied. A sliding-mode controller is applied on the linearized system. The inverse model of the system is used as an actuator for the direct system control. The simulated results show that this control method can be applied successfully to the linear systems control. Next, a full-state feedback controller is designed using the Lyapunov-Floquet transformation technique. For the controlled system, all states vanish before a new impact occurres. The system controller applies a large control torque immediately after the impact moment. The results obtained show that Lyapunov-Floquet transformation is a powerful tool for linear controllers design. Finally, a fuzzy-logic strategy is applied for nonlinear system control. This strategy does not require a priori knowledge of the equations of motion. The technique is simple and suitable for a real-time implementation.

References

1. **Beale, M.; Demuth, H.:** Fuzzy Systems Toolbox – For Use With MATLAB. Boston: PWS Publishing Company 1994
2. **Beale, D.; Lee, S. W.:** The applicability of fuzzy logic control for flexible mechanisms. pp. 203–210 ASME The 15th Biennial Conference on Mechanical Vibration and Noise, Boston, 84(1) 1995
3. **Berbyuk, V. E.:** On the controlled rotation of a system of two rigid bodies with elastic elements. PMM (U.S.S.R.) 48(2) (1984) 164–170
4. **Boghiu, D.; Marghitu, D. B.; Sinha, S. C.:** Fuzzy Logic Control of a Parametrically Excited Rotating Beam. J. Low Frequency Noise Vib. and Active Control (1998 in press)
5. **Cannon, R.; Schmitz, E.:** Initial experiments on the end-point control of a flexible one-link robot. Int. J. Robotics Res. 3(3) (1984) 62–75
6. **Crespo da Silva, M. R. M.; Glynn, C. C.:** Nonlinear-flexural-torsional dynamics of inextensional beams. II: Forced motions. J. Struct. Mech. 6 (1978) 449–461
7. **Crespo da Silva, M. R. M.; Glynn, C. C.:** Non-linear non-planar resonant oscillations in fixed-free beams with support asymmetry. Int. J. Solid Structures 15 (1979) 209–219
8. **Joseph, P.; Pandiyan, R.; Sinha, S. C.:** Optimal control of mechanical systems subjected to periodic loading via Chebyshev polynomials. Optimal Control Appl. Methods 14 (1993) 75–90

9. **Lim, C. M.; Hiyama, T.:** Application of fuzzy logic control to a manipulator. IEEE Transactions on Robotics and Automation 7(5) (1991) 688–691
10. **Marghitu, D. B.; Diaconescu, C.; Boghiu, D.:** Fuzzy-logic control of parametrically excited impacting flexible system. J. Appl. Mech. 68 (1997) 259–270
11. **Marghitu, D. B.; Diaconescu, C. I.:** Sliding mode control of an impacting elastic element using inverse model. J. Low Frequency Noise Vib. Active Control (1998) in press
12. **Marghitu, D. B.; Hurmuzlu, Y.:** Three-dimensional rigid-body collisions with multiple contact points. J. Appl. Mech. 62 (1995) 725–732
13. **Nathan, P. J.; Singh, S. N.:** Sliding mode control and elastic mode stabilization of a robotic arm with flexible links. J. Dyn. Syst. Meas. Control 113 (1991) 669–754
14. **Pfeiffer, F. Glocker, C.:** Multibody Dynamics with Unilateral Contacts. New York: J. Wiley & Sons 1996
15. **Silverman, L. M.:** Inversion of Multivariable Linear Systems. IEEE Trans. Aut. Control AC(14) (1969) 270–276
16. **Singh, T.; Golnarachi, M.; Dubey, R.:** Sliding mode/shaped input control of flexible/rigid link robot. J. Sound Vib. 171(2) (1994) 185–200
17. **Sinha S. C.; Joseph P.:** Control of general dynamic systems with periodically varying parameters via Lyapunov-Floquet transformation. ASME J. Dyn. Syst. Meas. Control 161 (1994) 650–658